www.sciencemag.org/cgi/content/full/313/5794/1765/DC1

Supporting Online Material for

Self-Healing Pulse-Like Shear Ruptures in the Laboratory

George Lykotrafitis, Ares J. Rosakis,* Guruswami Ravichandran

*To whom correspondence should be addressed. E-mail: Rosakis@aero.caltech.edu

Published 22 September 2006, *Science* **313**, 1765 (2006)
DOI: 10.1126/science.1128359

This PDF file includes:

Supporting Online Material

Self-healing, pulse-like, shear ruptures in the laboratory

George Lykotrafitis, Ares J. Rosakis, Guruswami Ravichandran*
Graduate Aeronautical Laboratories
California Institute of Technology (Caltech), Pasadena, CA 91125, USA

Materials and Specimen Configuration

Two identical incoherent Homalite plates, are subjected to uniform compressive stress and to dynamic shear loading. Each of the plates was $139.7\,\text{mm}$ long, $76.2\,\text{mm}$ wide and $9.525\,\text{mm}$ thick (Fig. S1b). Homalite-100 is a brittle polyester resin that exhibits stress-induced birefringence and is mildly rate-sensitive. At the strain rate developed during our experiments (on the order of $10^3\,\text{s}^{-1}$) and at room temperature, Homalite exhibits a purely linear elastic behavior. The pressure, shear and Rayleigh wave speeds of Homalite-100 are $C_P = 2187\,\text{m/s}$, $C_S = 1249\,\text{m/s}$ and $C_R = 1155\,\text{m/s}$ respectively. The asymmetric impact loading was imposed via a cylindrical steel projectile of diameter $25.4\,\text{mm}$ and length $50.8\,\text{mm}$, fired using a gas gun. The impact speeds ranged from $10\,\text{m/s}$ to $20\,\text{m/s}$. A steel buffer $73\,\text{mm}$ high, $25.4\,\text{mm}$ long and $9.525\,\text{mm}$ thick was attached to the impact side of the upper plate to prevent shattering and to induce a more or less planar loading wave.

Research methodology

Diagnostics

Dynamic photoelasticity, visualizing full-field contours of maximum shear stress, was combined with a laser interferometry-based technique, giving a local measurement of the sliding velocity at the interface (Fig. S1).

A typical dynamic photoelasticity experimental setup is shown in Fig. S1a. The contours (isochromatic fringes) of maximum in-plane shear stress τ_{max} are governed by the stress optical law $2\tau_{max} = \sigma_1 - \sigma_2 = N F_\sigma / h$ where F_σ is the material's stress optical coefficient, h is the specimen thickness, σ_1, σ_2 are the principal stresses and $N = n + 1/2$ (with $n = 0,1,2,..$) is the isochromatic fringe order (*S1*). Since this technique is sensitive to maximum shear stresses, it is very well suited for the study of dynamic shear rupture. The evolution of the isochromatic fringe pattern was recorded by a high speed digital camera (Cordin model 220). The recording frame rate for most of the experiments was 1 frame per $4\mu s$. A collimated laser beam with a diameter of 130 mm was used to illuminate most of the specimen.

A pair of independent velocimeters was used to continuously measure the horizontal particle velocities at two adjacent points M_1 and M_2 across the interface (Fig. S1B). The results were registered on submicro-second time-scales. The velocimeter consists of a

modified Mach-Zehnder fiber-optic interferometer and a velocity decoder. The decoder was set to a full range scale of $\pm 10\,\mathrm{m/s}$ with a maximum frequency of $1.5\,\mathrm{MHz}$ and a maximum acceleration of $10^7\,\mathrm{g}$. The experimental error was on the order of 1%. The horizontal relative velocity history was obtained by subtracting the velocity of the point below the interface (M_1) from that of the point above the interface (M_2). The technique and the corresponding experimental setup is presented in detail in Lykotrafitis, Rosakis and Ravichandran (*S1*).

Establishing the onset of sliding and the arrival of the rupture tip

The procedure we pursued to pinpoint the time at which we conjectured that the sliding started at the relative velocity measurement location is the following. We first observed the photoelastic figures which often show the arrival of the rupture tip at the velocity measurement points. Photoelasticity and high-speed photography are always helpful in identifying the rupture tip arrival time to within 5%. Since the photoelastic and velocity measurements were synchronized, we next narrowed down the above time interval by observing the relative velocity history and identifying the time for which this velocity increased dramatically for the first time within that interval. Then, we used the above time to establish the relative horizontal velocity level which corresponds to sliding initiation at this particular experiment. This establishes the level of the horizontal dashed line in our velocity figures.

As an example, we will apply the above procedure on an experimental result which has not appeared in the submitted paper but we include it in the online material (Fig. S3). In this case the static pre-stress was10 MPa as in all cases in the manuscript but the impact speed was 24 m/s, higher than the impact speeds that appeared in the manuscript. Fig. S3a displays a photoelastic fringe pattern captured approximately at 40 μs after the synchronous triggering of the camera and the interferometers. The photoelastic image shows that the leading photoelastic fringe structure reached the velocity measurement position at 40 μs. The P-wave front arrived there earlier since it was ahead of the fringe structure but it is not visible in this case because photoelasticity is not sensitive in volumetric changes. The photoelastic image in Fig. S3b reveals that the fringe concentration point A (tip of the Mach cone), which in classical shear crack propagation experiments signifies the rupture initiation, arrived at the velocity measurement positions M_1 and M_2 at approximately 50 μs, (the sliding tip was traveling at a super-shear speed of 1.3 C_S creating a Mach cone). Thus, we have identified so far, within an experimental error of 5%, in time the arrival of the P-wave and of the fringe concentration point at the relative velocity measurement position. We next focus our attention to the Fig. S3c which shows the velocity histories of points M_1 in the lower plane (blue line) and point M_2 in the upper plane (red line) as well as the relative velocity history (green line). From the velocity measurements is clear that the P-wave front arrived at the velocity measurement position at approximately 37 μs (Fig. S3c), since at this time both points started to displace together. Furthermore, Fig. S3c shows that points M_1 and M_2 traveled together at the same speed from approximately 37 μs until approximately 45 μs when a small difference in their velocity started to appear. The relative velocity however, remained small until the 50.5 μs when it underwent a huge change. The above time is correlated

very well with the arrival of the fringe concentration point A (tip of the Mach cone) at the measurement position.

Now, let us look at the evolution of the relative displacement (time integral of the relative velocity history) between points M_1 and M_2 from 35 μs (just before the arrival of the P-wave) until 50.5 μs (Fig. S3d). The relative horizontal displacement until 50.5 μs, just before the arrival of the fringe concentration point at points M_1 and M_2, was 1.5 μm, much smaller than the vertical distance between points M_1 and M_2 which was approximately 500 μm. The resulting shear strain was approximately 0.3 % which in the case of an intact Homalite plate lies in the elastic regime. Taking into consideration all of the above information, we conjecture that the interface was locked until 50.5 μs. Subsequently, the sliding started, and the rupture was represented by fringe concentration point A. The relative displacement of 1.5 μm is only a result of elastic deformation in the material between the two measurement points. At 50.5 μs the arrival of the sliding tip resulted in a huge increase of the relative velocity (Fig. S3c). We believe that this is the beginning of sliding and we substantiate that through the visible arrival of the Mach cone at that location at approximately 50 μs as shown in Fig. S3b.

Following the same argument as above, we conjecture that the deformation in Fig. 1B until 13 μs (when the velocity (Fig. S4a) increased sharply) was elastic, since the relative deformation up to this point was approximately 2 μm (Fig. S4b), which corresponds to approximately 0.4 % shear strain. The sliding started when the fringe concentration point A arrived at the velocity measurement positions.

Establishing that healing has taken place in "pulse-like" sliding situations
When "pulse-like" behavior takes place, we make the assumption that the sliding speed on the interface near the back end of the pulse decreases and drops very close to zero if the relative velocity between points M_1 and M_2 has dropped to the non-zero level established by the dashed line. Below that level we conjecture that a stationary contact has been established and that the recorded relative velocity is only due to elastic shear deformation between points M_1 and M_2 (500 μm apart).

To illustrate this point as clearly as we can, we exploit the figure S5. In that figure, the entire horizontal velocity histories of points M_1 and M_2 as well as the relative displacement history are added to the velocity history shown in Fig. 2D of the manuscript. In the Fig. S5a, a dashed line crosses the relative velocity (green line) for the first time at 58 μs. This time and the associated dashed line are established through the procedure outlined above. The total relative displacement between points M_1 and M_2 up to that point was approximately 2.5 μm (Fig. S5b). Following the same argument as in the cases shown in Figs. S3 and S4, we conjecture that up to this point there was no slip but only elastic shear deformation of the material between points M_1 and M_2. It is now interesting to follow the evolution of the relative velocity (green line in Fig. S5a) in relation to the evolution of the relative displacement (Fig. S5b). The relative velocity increased sharply after the initiation of sliding and then decreased. At 65 μs it reached the same velocity of approximately 0.7 m/s, which was the relative velocity of points M_1 and M_2 just after the sliding initiation (dashed line level). The relative displacement history

(Fig. S5b) shows that from 64 μs until 65 μs the relative displacement accumulation (0.7 μm) was very small. We conjecture that while the distance between points M_1 and M_2 increased (although very little) the asperities in contact were locked for the above period of 1 μs and they again separated abruptly at 65 μs. It is characteristic that the change in the relative velocity at 65 μs follows the same trend with the sharp increase of the relative velocity at the initiation of the crack-like sliding (Fig. 1 and Fig. S4).

Reference

S1 G. Lykotrafitis, A. J. Rosakis, G. Ravichandran, *Exper. Mech.* **46**, 205 (2006).

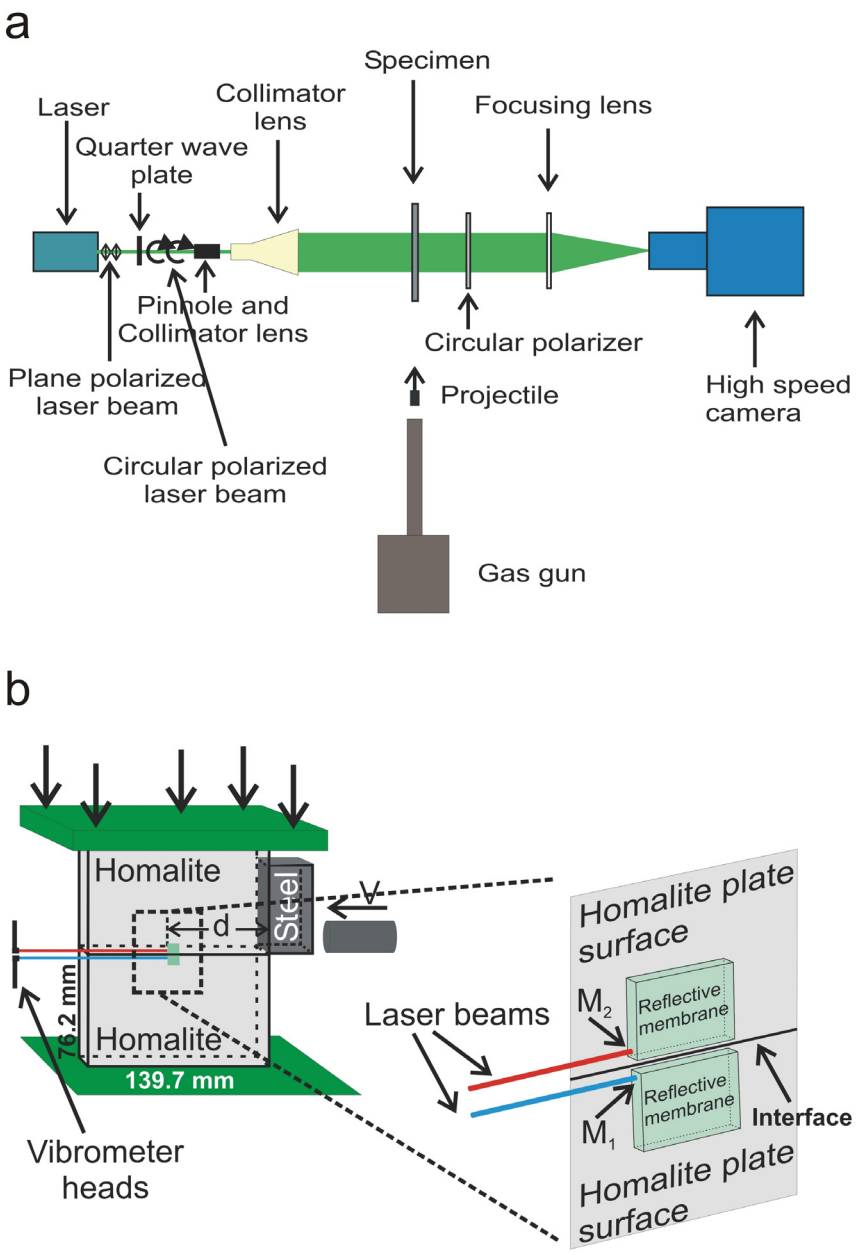

Fig. S1: (a) A typical dynamic photoelasticity experimental setup combined with a high-speed digital camera. (b) Two identical incoherent Homalite plates are subjected to uniform compressive stress and to dynamic shear loading imposed via a cylindrical steel projectile. A pair of independent fiber-optic velocimeters was used to continuously measure the horizontal particle velocities at two adjacent points M_1 and M_2 across the interface. By subtracting the velocity of the point below the interface (M_1) from that of the point above the interface (M_2), the horizontal relative velocity history was obtained.

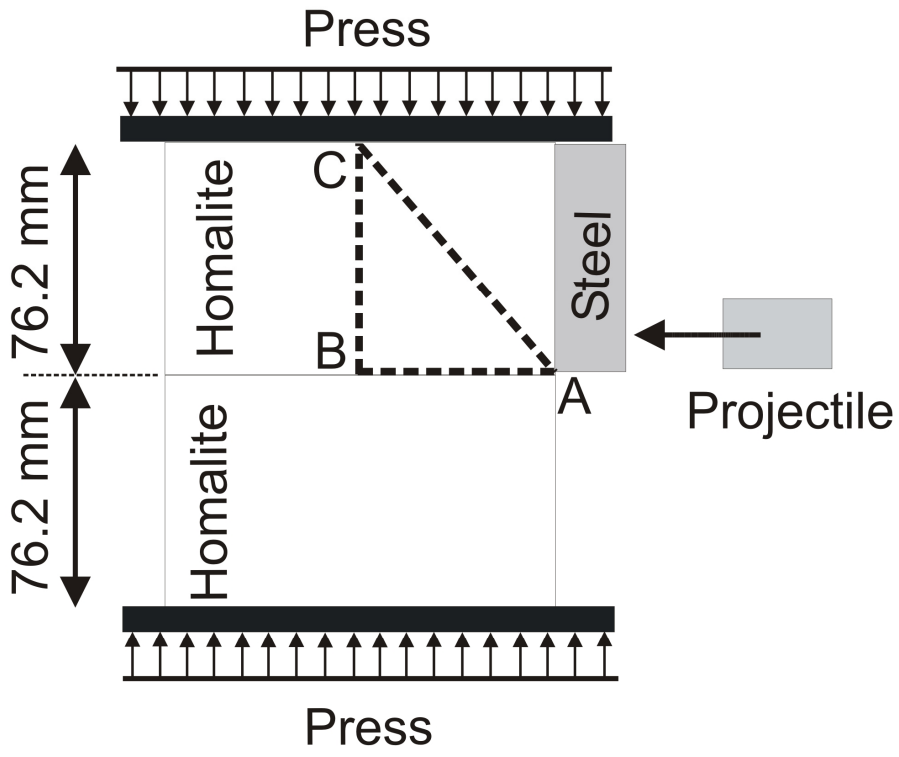

Fig. S2: Two identical Homalite plates are subjected to uniform compressive stress and to dynamic shear loading imposed via a cylindrical steel projectile. Two possible approximate ray paths for P-waves transmitted from the buffer (point A) to the velocity measurement position B are shown. Path ACB corresponds to a P-wave reflected at point C on the top plate of the press while path AB corresponds to a P-wave directly transmitted to point B from point A. The differences in the arrival times of the P-waves, which traveled at a speed of 2187 m/s, were approximately 50 μs and 59 μs for the cases of AB = 70 mm and AB = 30 mm respectively.

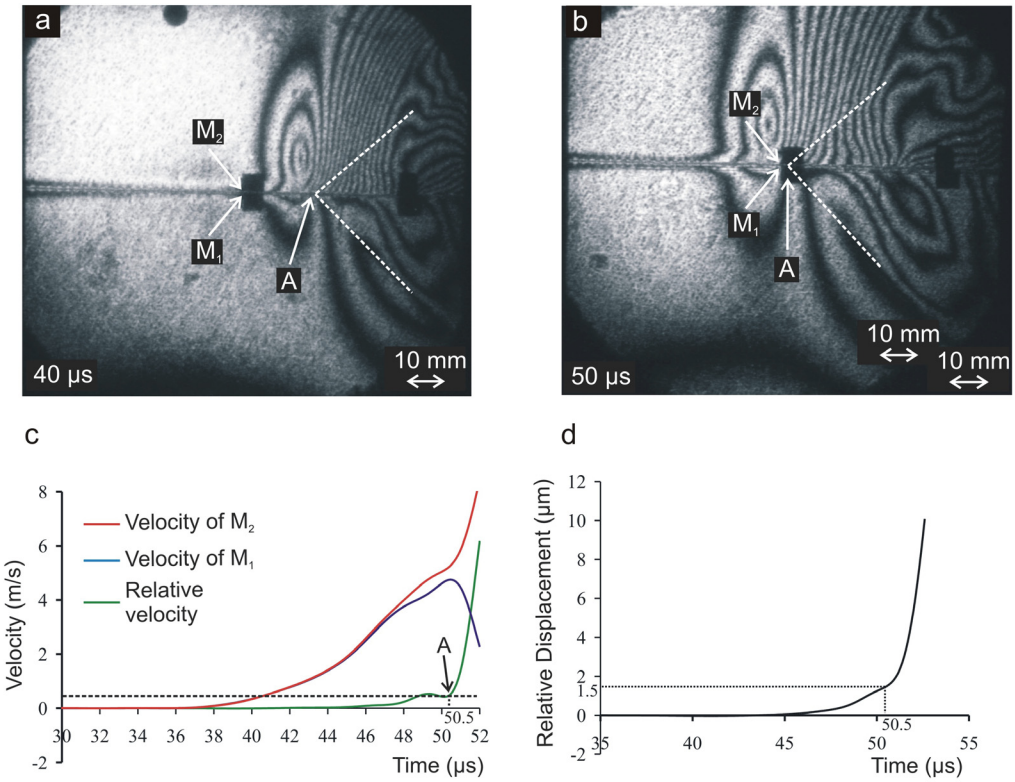

Fig. S3 The figure illustrates how the synchronized photoelastic and velocimetry measurements are used to identify the arrival of the rupture tip. (a) and (b) Isochromatic fringe patterns captured at 40 μs and 50 μs respectively after impact. The external uniform compression was 10 MPa and the impact speed was 24 m/s. The rupture tip is at the fringe concentration point A. The dotted lines highlight the location of the Mach lines emanating from the rupture tip. (c) Horizontal velocity histories and relative horizontal velocity history of points M_1 and M_2 located 70 mm from the impact side of the Homalite plate. The rupture commenced when the rupture tip A reached the velocity measurement position at 50. 5 μs. (d) Relative horizontal displacement history of points M_1 and M_2.

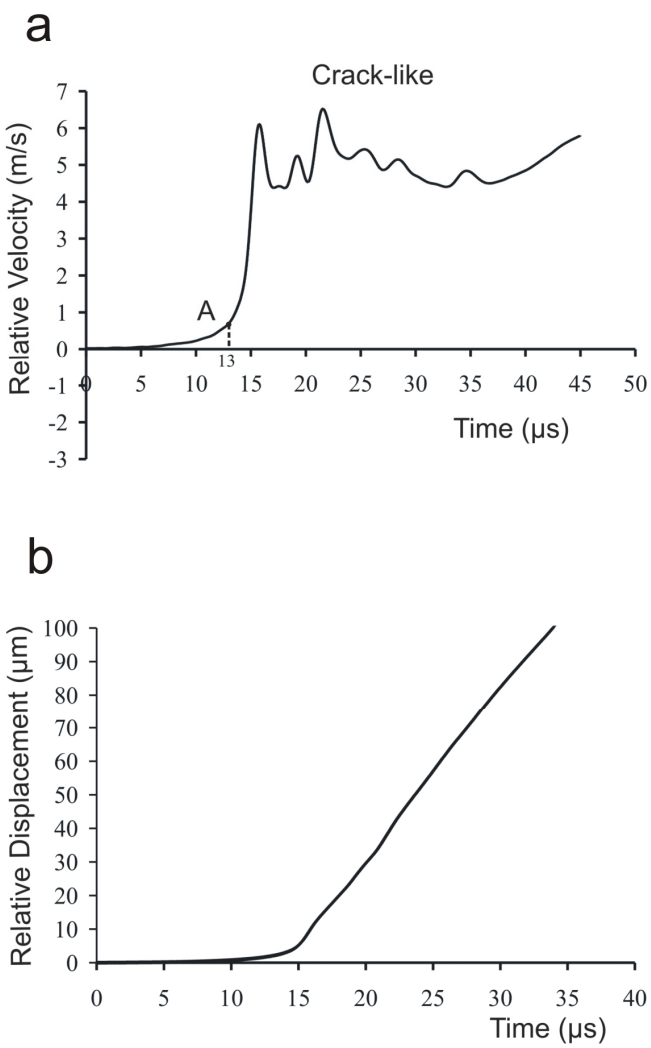

Fig. S4: (a) Relative velocity history of points M_1 and M_2 which belong to the upper and lower plate respectively and are located at a distance of 70 mm from the impact side of the Homalite plates. The static pre-stress was 10 MPa. The rupture commenced when the rupture tip A reached the velocity measurements position at 13 μs (b) Relative horizontal displacement history of points M_1 and M_2.

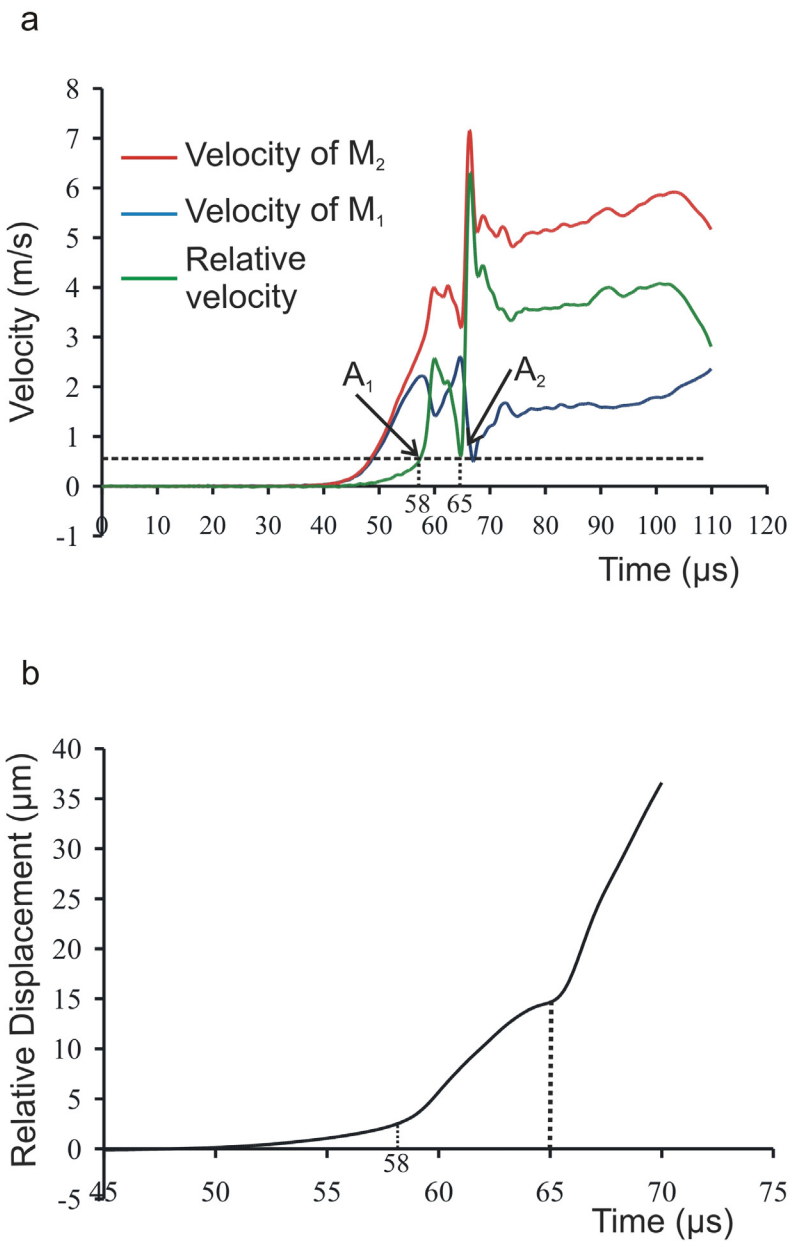

Fig. S5: (**a**) Horizontal velocity histories and relative horizontal velocity history of points M_1 and M_2 located 30 mm from the impact side of the Homalite plate. The rupture commenced when the rupture tip A reached the velocity measurement position at 58 μs (A_1) and it resumed at 65 μs (A_2). (**b**) Relative horizontal displacement history of points M_1 and M_2.